



## Modeling Extracellular Matrix Degradation Balance with Proteinase/ Transglutaminase Cycle

VÉRONIQUE LARRETA-GARDE<sup>†</sup> AND HUGUES BERRY<sup>\*†</sup>

<sup>†</sup>*Equipe de Recherche sur les Relations Matrice Extracellulaire-Cellules (ERRMECe), Université de Cergy-Pontoise, 2 Avenue A. Chauvin, BP 222, 95302 Cergy Pontoise Cedex, France*

(Received on 22 October 2001, Accepted in revised form on 4 March 2002)

Extracellular matrix mass balance is implied in many physiological and pathological events, such as metastasis dissemination. Widely studied, its destructive part is mainly catalysed by extracellular proteinases. Conversely, the properties of the constructive part are less obvious, cellular neo-synthesis being usually considered as its only element. In this paper, we introduce the action of transglutaminase in a mathematical model for extracellular matrix remodeling. This extracellular enzyme, catalysing intermolecular protein cross-linking, is considered here as a reverse proteinase as far as the extracellular matrix physical state is concerned. The model is based on a proteinase/transglutaminase cycle interconverting insoluble matrix and soluble proteolysis fragments, with regulation of cellular proteinase expression by the fragments. Under “closed” (batch) conditions, i.e. neglecting matrix influx and fragment efflux from the system, the model is bistable, with reversible hysteresis. Extracellular matrix proteins concentration abruptly switches from low to high levels when transglutaminase activity exceeds a threshold value. Proteinase concentration usually follows the reverse complementary kinetics, but can become apparently uncoupled from extracellular matrix concentration for some parameter values. When matrix production by the cells and fragment degradation are taken into account, the dynamics change to sustained oscillations because of the emergence of a stable limit cycle. Transitions out of and into oscillation areas are controlled by the model parameters. Biological interpretation indicates that these oscillations could represent the normal homeostatic situation, whereas the other exhibited dynamics can be related to pathologies such as tumor invasion or fibrosis. These results allow to discuss the insights that the model could contribute to the comprehension of these complex biological events. © 2002 Elsevier Science Ltd. All rights reserved.

### 1. Introduction

The extracellular matrix (ECM) is an insoluble mesh of various structural and functional macromolecules encountered in connective tissues and basement membranes. It constitutes both a barrier separating organisms into tissue compartments and a substratum for cell adhesion (Price *et al.*, 1997). Besides this

structural role, the ECM is an essential regulator of cell physiology, predominantly implied in morphogenesis, cell survival, cell cycle, cell migration and tumorigenesis (Basbaum & Werb, 1996). During normal maintenance or pathological modifications, the ECM undergoes intense cell-controlled composition changes. This process, called ECM “remodeling”, is involved in many physiological processes such as embryogenesis (Hay, 1981; Perris & Perissinotto, 2000), immune cell activation (Dustin &

\*Corresponding author. Fax: +33-134-25-65-52.  
E-mail address: [hugues.berry@bio.u-cergy.fr](mailto:hugues.berry@bio.u-cergy.fr) (H. Berry).

de Fougerolles, 2001), reproductive cycles (Hullboy *et al.*, 1997), wound healing (Witte & Barbul, 1997; Davis *et al.*, 2000) or neo-angiogenesis (Liotta *et al.*, 1991).

Among the pathologies involving abnormal ECM remodeling, metastasis dissemination has received highest interest. To disseminate, a tumor cell must cross several ECM layers (interstitial ECM, basement membranes beneath endothelia) that otherwise are impermeable to most cell types (tissue invasion). To this end, invasive cells are thought to use specific proteinases, among which the most studied are matrix metalloproteinases (MMPs) and the plasmin/plasminogen activator pair (for recent reviews, see Murphy & Gavrilovic, 1999; DeClerck, 2000; or McCawley & Matrisian 2000). Although many points still remain unclear (McCawley & Matrisian 2001), the major rationale is that proteolysis would disorganize ECM assembly in a way that makes it permeable to cells. In agreement with this hypothesis, numerous ECM-degrading proteinases have been correlated with tumor invasiveness or metastatic potential (Nakahara *et al.*, 1997; Cockett *et al.*, 1998). Moreover, knock-out experiments on proteinase genes (Wilson *et al.*, 1997) or administration of specific inhibitors (Denis & Verweij, 1997; Duffy & McCarthy, 1998) have further established the involvement of these enzymes in tumor dissemination.

Transglutaminase is another extracellular enzyme implicated in ECM remodeling that catalyses the formation of an intermolecular covalent bond between a glutamine and a lysine residue of two proteins (Folk *et al.*, 1967). Despite its involvement in cell adhesion (Corbett *et al.*, 1997), migration (Akimov & Belkin, 2001; Belkin *et al.*, 2001) and cancerogenesis (Haroon *et al.*, 2000; Grigoriev *et al.*, 2001), it has received considerably less interest than proteinases. Yet, transglutaminase is known (and industrially used) for its ability to modify the rheological properties of biological media (Nio *et al.*, 1986; Motoki & Seguro, 1998). Protein cross-linking enhances viscosity and can lead to formation of an insoluble gel from a protein solution. In the ECM also, transglutaminase contributes to the unsolubilization of the protein lattice and is accordingly implied in ECM

remodeling (Aeschlimann & Thomazy, 2000). In other words, whereas proteinases disorganize the ECM via partial solubilization (Berry *et al.*, 2000), transglutaminase contributes to reorganizing it, creating insoluble matrix from soluble fragments.

Cell-ECM interactions form a complex and nonlinear system that can manifest non-trivial or emergent properties. Theoretical modeling is thus an important task in the way to its understanding. An informative example is the model of DiMilla *et al.* (1991), that has predicted the now widely accepted biphasic dependence of cell migration speed on ECM adhesiveness even before it was confirmed by experimental observation (Palecek *et al.*, 1997).

In this paper, we present a mathematical model for ECM remodeling balance, that includes the counteracting actions of transglutaminase and proteinase (futile cycle) and some of the consequences of cell signaling in response to ECM stimulation. The next section provides a general description of the model, and presents the ordinary differential equations of its mathematical formulation. Section 3 gives experimentally based variation ranges for the values of some of the parameters. The model is then studied in two different cases. In the first (Section 4), we study the “closed” (batch) version of the model, i.e. with no ECM or proteolysis fragment influx or efflux from the system, and show that in this case, the system exhibits bistability with accompanying threshold and memory properties. In the next section (Section 5), we present the study of the model in “open” conditions, i.e. with ECM influx and proteolysis fragments efflux. We show that the dynamics are profoundly altered, with the emergence of a limit cycle generating sustained oscillations of the ECM concentration and proteinase concentration. Finally, we conclude with a discussion of application to cell invasion and more general ECM remodeling in the last section (Section 6).

## 2. General Description of The Model

A schematic representation of our model is shown in Fig. 1. ECM proteins solubilization is achieved via peptide bonds hydrolysis catalysed

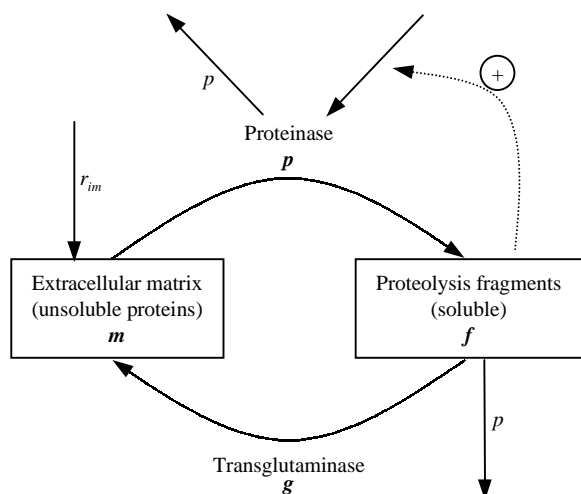


FIG. 1. Scheme of the proposed model for ECM synthesis and degradation. Indicated with slanted letters are the variables representing the concentrations of the corresponding molecular species. Unsoluble ECM proteins ( $m$ ) are produced by cells at constant rate  $r_{im}$  and degraded by proteinases ( $p$ ) into soluble proteolysis fragments ( $f$ ). Fragments can be cross-linked by transglutaminase ( $g$ ) or other intermolecular protein-cross-linking enzyme to yield back new unsoluble ECM proteins. Fragments are subject to proteolysis from  $p$  and interact with cells to increase proteinase concentration (positive feedback loop, dashed arrow). Proteinases themselves undergo autoproteolysis.

by proteinases. As the nature of the substrate (ECM proteins) is not specified in our model, proteinase specificity does not come into consideration. The term “proteinase” thus designates any ECM proteinase. The reverse reaction is covalent intermolecular protein crosslinking and is catalysed by transglutaminase (or any protein-crosslinking enzyme). Inasmuch as this reaction contributes to ECM unsolubilization from soluble protein fragments, transglutaminase’ effect on ECM solubility can be considered as the reverse of proteinase influence. In our model, proteinases and transglutaminases become the two antagonist catalysts of a futile cycle between ECM proteins and their proteolysis fragments. Both enzymes are assumed to display Michaelis–Menten kinetics with  $k_p$  and  $k_g$  as the catalytic constants and  $K_P$  and  $K_G$  the Michaelis constants for proteinase and transglutaminase, respectively. Proteinase-catalysed degradation of the fragments is also taken into account. For simplicity, we assume that the kinetic constants for this reaction are the same as

those for unsoluble matrix protein proteolysis (i.e.  $k_p$  and  $K_P$ ).

Matrix metalloproteinases are subject to autoproteolytic inactivation. Autoproteolysis is usually a multistep process that consists of one or several enzyme conformational changes. One of these conformations is a substrate for the active enzyme (autoinactivation or autoactivation) or an active form that uses the native zymogene as a substrate (autoactivation). This is, for example, the case of the human complement subcomponent C1r autoactivation (Villiers *et al.*, 1983; Kasahara *et al.*, 1985) or of the autocatalytic step of matrix metalloproteinase-2 activation (Atkinson *et al.*, 1995; Will *et al.*, 1996; Morugovna *et al.*, 1999). For simplification, we choose to neglect any conformational change, and consider autoproteolysis as the catalytic activity of one enzyme molecule onto another enzyme molecule. Formally, we treat this enzyme activity as a Michaelis-type behavior, with  $k_{deg}$  and  $K_{deg}$  the catalytic and Michaelis constants, respectively. Proteinase is thus both the enzyme and its substrate of autoproteolytic inactivation. Possible transglutaminase deactivation through proteolysis is omitted, so that transglutaminase concentration remains constant in our model and is considered as a parameter.

*In vivo*, cells perceive and regulate the characteristics of the surrounding ECM using several membrane receptors that specifically recognize ECM elements. These receptors provide cells with responses to ECM physical and chemical changes by modulating signal-transduction cascades into the cells. These intracellular cascades control the production of a wide range of proteins, which, in turn, can modify ECM or cell physiology (LaFlamme & Auer, 1996; Yamada, 1997). This so-called “outside-in” signaling thus allows a permanent and bidirectional dialogue between cells and ECM. For instance, modulation of proteinase expression by the cells in response to ECM modifications has been well documented and is a crucial event in metastasis dissemination (Liotta *et al.*, 1991; Werb, 1997; Crowe & Shuler, 1999). In fibroblasts, proteolysis fragments of fibronectin (an ECM protein) induce expression and secretion into the ECM of neo-synthesized

proteinases, whereas the entire fibronectin molecule does not (Werb *et al.*, 1989). Fragment production thus tends to enhance proteinase concentration and consequently, fragment concentration, creating an indirect positive feedback loop.

This is taken into account in our model by assuming that the rate of proteinase concentration change partly depends on fragment concentration. To describe the effect of proteolysis fragments on proteinase concentration, we assumed that many molecular events involved in this feedback loop may possibly display ultrasensitive switch-like kinetics (Goldbeter & Koshland, 1982). For instance, some of the molecular systems triggering signal transduction from ECM receptors are kinase/phosphatase cycles (LaFlamme & Auer, 1996; Bouvard *et al.*, 1998), which are known to exhibit nonlinear sigmoid responses to input signals both theoretically (Huang & Ferrell, 1996) and experimentally (Bagowski & Ferrell, 2001). More specifically, the secretion by mammalian cells of the gelatinase B MMP, in response to phorbol esters, has recently been shown to be switch-like both theoretically and experimentally (Marique & Wérenne, 2001). Accordingly, we assume in our model a Hill equation for the dependence of proteinase concentration change on fragment concentration, with  $\alpha$  as the maximum rate,  $K_R$  the threshold constant and  $n$  the Hill number. Furthermore, the model also incorporates ECM production by the cells at a constant rate  $r_{im}$ . Thus, although the presence of cells is not explicitly included, cellular regulation of the considered ECM elements is incorporated in the model.

Designating  $p$ ,  $m$  and  $f$ , the time-dependent concentrations of proteinase, ECM proteins, and their corresponding fragments, respectively, and  $g$ , the transglutaminase concentration, we obtain a set of three ordinary differential equations

$$\frac{dm}{dt} = -k_p p \frac{m}{K_P + m} + k_g g \frac{f}{K_G + f} + r_{im}, \quad (1a)$$

$$\frac{df}{dt} = k_p p \frac{m}{K_P + m} - k_g g \frac{f}{K_G + f} - \delta k_p p \frac{f}{K_P + f}, \quad (1b)$$

$$\frac{dp}{dt} = \alpha \frac{f^n}{K_R^n + f^n} - k_{deg} \frac{p^2}{K_{deg} + p}, \quad (1c)$$

where the parameter  $\delta$  [eqn (1b)] has been added for convenience: its value is 1 if fragment's ( $f$ ) proteolysis is taken into account, and is 0 in the other case. The numerator of the second term in the right-hand side of eqn (1c) (autoproteolytic inactivation term) contains a  $p^2$  term, that originates from the fact that  $p$  represents both the enzyme and the substrate during autoproteolysis, described here as Michaelis–Menten kinetics.

We then non-dimensionalize the system [eqn (1)] by normalizing each variable  $p$ ,  $g$ ,  $m$  and  $f$  by  $K_P$  and time by  $1/k_p$ , and obtain the dimensionless system

$$\frac{dm}{dt} = -p \frac{m}{1+m} + k_g g \frac{f}{K_G + f} + r_{im}, \quad (2a)$$

$$\frac{df}{dt} = p \frac{m}{1+m} - k_g g \frac{f}{K_G + f} - \delta p \frac{f}{1+f}, \quad (2b)$$

$$\frac{dp}{dt} = \alpha \frac{f^n}{K_R^n + f^n} - k_{deg} \frac{p^2}{K_{deg} + p}, \quad (2c)$$

where concentrations ( $p$ ,  $g$ ,  $m$ ,  $f$ ,  $K_G$ ,  $K_R$  and  $K_{deg}$ ) are in  $K_P$  units, first-order rate constants ( $k_g$  and  $k_{deg}$ ) are in  $k_p$  units, rates ( $r_{im}$  and  $\alpha$ ) are in  $K_P \times k_p$  units and time is in  $1/k_p$  units.

### 3. Parameter Values

Biologically relevant variation ranges for some parameters of eqn (2) can be stated.  $k_p$  and  $K_P$  have been determined for a variety of ECM proteinases, especially matrix metallo proteinases (MMPs). These kinetic parameters vary with the substrate and the enzyme, but for human type-I collagenase (MMP1) on human collagen substrates,  $k_p$  can be estimated to vary between 50 and 500  $\text{hr}^{-1}$  and  $K_P$  is of the order of 1  $\mu\text{M}$  (Birkedal-Hansen *et al.*, 1993). As far as transglutaminase is concerned, data from the literature are not easy to exploit, because the assumed kinetic mechanism is usually the bisubstrate ping-pong type, and not the simple monosubstrate Michaelis one, as it is used in our

model (Folk, 1967). However, considering the values obtained, it can be generally stated that transglutaminases are less active enzymes than proteinases, but exhibit greater affinities for their substrates (Chung *et al.*, 1970; Leblanc *et al.*, 2001). In terms of the dimensioned, natural parameter, we shall thus consider  $k_p > k_g$  and  $K_P > K_G$ , or with the dimensionless ones:  $k_g < 1$  and  $K_G < 1$ .

Autoproteolysis is a classical proteolysis event, except for its substrate that consists in the enzyme itself. However, for the sake of efficiency we would not expect the enzyme to be a better substrate than its naturally encountered one. We shall thus generally assume:  $k_{deg} \leq k_p$  and  $K_{deg} \geq K_P$  (natural parameters) or  $k_{deg} \leq 1$  and  $K_{deg} \geq 1$  (dimensionless parameters). The remaining parameters ( $\alpha, r_{im}, K_R$ ) could not be estimated and were usually varied here between  $10^{-3}$  and  $10^3$  (in dimensionless form).

#### 4. “Closed” Model

In this section we study a simplified version of eqn (2) that we can analyse in two-dimensional phase space. It is obtained by setting  $r_{im} = \delta = 0$  in eqn (2), i.e. by neglecting ECM protein entry or fragment exit through proteolysis from the system (as in a batch reactor). The global concentration (matrix protein + fragment) is thus conserved:  $m(t) + f(t) = m(0) + f(0) \equiv c_0$ . This constraint allows the reduction of the number of equations and eqn (2) reads

$$\frac{df}{dt} = p \frac{c_0 - f}{1 + c_0 - f} - k_g g \frac{f}{K_G + f}, \quad (3a)$$

$$\frac{dp}{dt} = \alpha \frac{f^n}{K_R^n + f^n} - k_{deg} \frac{p^2}{k_{deg} + p}. \quad (3b)$$

This simplified version resembles classical models for futile cycles with nonlinear negative feedback, such as kinase–phosphatase cycles (Lisman 1985; Ferrel & Xiong, 2001). These models are known to exhibit multistability properties (Laurent & Kellershohn, 1999). The major difference here lies in the indirect nature of the feedback loop that acts through proteinases. However, multistability originates from the model’s logical structure and is thus largely

independent of the system’s details (Thomas, 1998).

A trivial fixed point of eqn (3) is  $(f_0, p_0) = (0, 0)$  and will be referred to as “FP1”. It corresponds to a “matrix only” situation, i.e. a situation with maximal ECM concentration and without proteinase (nor proteolysis fragment). A plot of the nullclines (Fig. 2) of eqn (3) in the  $f$ – $p$  phase-space shows that, for some parameter values, two other fixed points (labeled “FP2” and “FP3” in Fig. 2) can coexist with FP1. Figure 3 shows the bifurcation diagram obtained with  $k_g g$  as a control parameter. For convenience, we represent ECM proteins ( $m$ ) evolutions as deduced from eqn (3) as  $m(t) = c_0 - f(t)$ . As inferred, FP1 value does not depend on  $k_g g$ . The eigenvalues of the Jacobian matrix evaluated at this fixed point are  $(\lambda_1, \lambda_2) = (0, -k_g g / K_G^2)$ , i.e. FP1 is a degenerate node for the linearized system. Inspection of graphic representations of the vector field as well as thorough numerical integrations indicates that this fixed point is stable (although “weakly”) for  $k_g g / K_G^2 \gg 1$ , but unstable for  $k_g g / K_G^2 = 0$ , in agreement with the non-zero eigenvalue. The first saddle-node bifurcation (fusion of the FP1 and FP2 branches) seems to be located to a small but non-zero parameter value. Nevertheless, FP1 being a degenerate node whose non-zero eigenvalue is proportional to the control parameter  $k_g g$ , its stability at very low control parameter values is poorly defined in the absence of a Lyapunov function. Furthermore, the unstable FP2 branch approaches the bifurcation tangentially to the FP1 one. This further complicates the exact localization of the bifurcation by numerical ways. The two other possible fixed points, FP2 and FP3, both exist at intermediate  $k_g g$  values only with FP2 unstable and FP3 stable. In contrast to FP1, FP3 is an “ECM-poor” fixed point where ECM has been widely degraded and proteinase and fragment concentrations are high.

Figure 3 characterizes a bistable behavior that we exemplify in Figs 4 and 5. Figure 4 presents ECM evolution  $m(t)$  with maximal initial ECM concentration [ $m(0) = c_0$ ], and variable initial proteinase concentrations  $p(0)$ . As long as  $p(0)$  is lower than a threshold concentration, the system remains asymptotically in the FP1

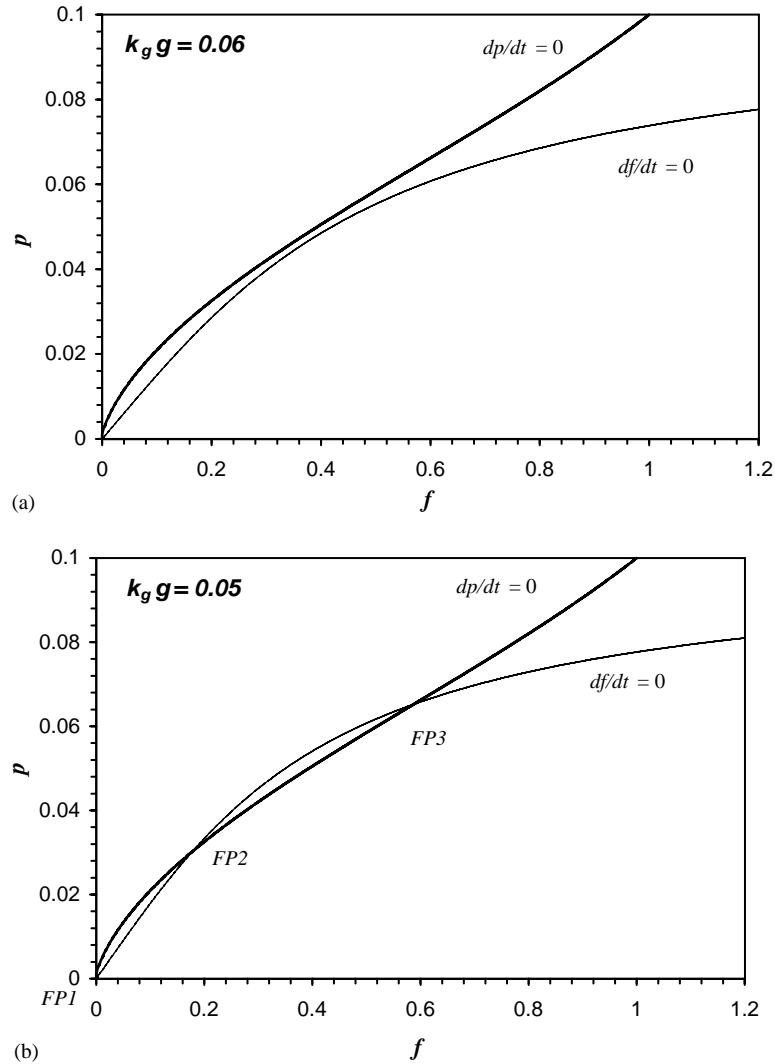


FIG. 2. Nullclines  $df/dt = 0$  (thin line) and  $dp/dt = 0$  (thick line) for the closed model [eqn (3)] in the  $f-p$  phase plane with  $k_g g = 0.06$  (a) or  $0.05$  (b). Other parameter values are:  $K_G = K_R = 0.1$ ;  $K_{deg} = 1$ ;  $k_{deg} = 0.1$ ;  $n = 3$ ;  $\alpha = 0.1$ ;  $c_0 = 0.1$  and  $r_{im} = \delta = 0$ . The fixed points are the intersections of the curves and are labeled “FP1”, “FP2” and “FP3” in (b).

“matrix-only” state. This clearly demonstrates the resistance of the system to proteinase’s attack of the matrix. We note that this resistance is caused by auto-regulation of the dynamical system and not by ECM protein’s protection or proteinases inhibition. Nevertheless, when proteinase concentration is high enough to reduce ECM concentration below FP2, the system switches to the other stable fixed point FP3, i.e. an “ECM-poor” state. This threshold effect is illustrated by curves 2 and 3 of Fig. 4, where initial proteinase concentration differs by less than 0.05%. Still, this is enough to switch from a high-ECM/zero-proteinase state to a low-

ECM/high-proteinase one. Furthermore, as can be seen in Fig. 4, bistability also implies that FP1 and FP3 are the only accessible states at long times, excluding any other intermediate state.

In bistable systems, transition from one stable fixed point to another one displays memory properties (hysteresis). This is illustrated in Fig. 5 where eqn (3) integration is initiated with a low  $k_g g$  (transglutaminase activity) value and is close to the “ECM-poor” state (FP3). The model equations are integrated for 200 time units with  $k_g g = 0.02$ .  $k_g g$  is then abruptly increased to 0.04 at  $t = 200$ , and the equations integrated for the next 200 time units, keeping this  $k_g g$  value

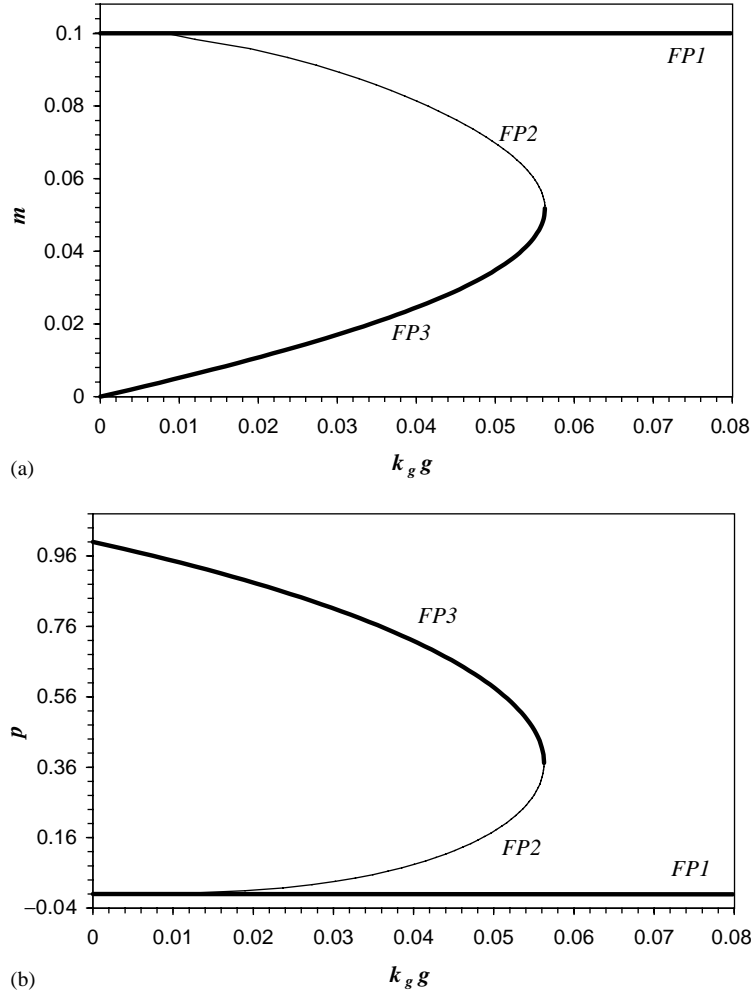


FIG. 3. Bifurcation diagrams showing the evolution of  $m$  (a) and  $p$  (b) components of the three fixed points (FP1, FP2 and FP3), with  $k_g g$  (transglutaminase activity) as the control parameter. Bold lines represent stable branches, thick lines are unstable ones. Note that the stability of FP1 for very low  $k_g g$  values as well as the location of the FP1–FP2 saddle-node bifurcation could not be ascertained (see text), except for  $k_g g = 0$  (where FP1 is unstable). The bold line for such very low values is thus a presentation convenience. Parameter values are:  $K_G = K_R = 0.1$ ;  $K_{deg} = k_{deg} = 1$ ;  $n = 3$ ;  $\alpha = 1$ ;  $c_0 = 0.1$  and  $r_{im} = \delta = 0$ . Continuation analysis of eqn (3) was performed with the program AUTO (Doedel, 1981) complemented with numerical analysis with SCILAB (<http://www-rocq.inria.fr/scilab/>).

constant. This process is iterated with gradually higher  $k_g g$  values, up to a final value of 0.10 (at  $t = 800$ ). The system remains on the FP3 branch while  $k_g g$  is lower than its threshold value (the value at the FP2–FP3 saddle-node bifurcation, i.e.  $\approx 0.056$ , see Fig. 3) and suddenly switches to the FP1 “ECM-rich” branch for higher (increasing) transglutaminase activities. When  $k_g g$  is then decreased back (from  $t = 1000$  in Fig. 5), the system remains on the FP1 branch until  $k_g g = 0$  ( $t = 1600$ ), even with  $k_g g$  values lower than the FP2–FP3 saddle-node bifurcation (0.056). Without transglutaminase, FP1 is un-

stable so that the system switches to the FP3 branch at  $k_g g = 0$ . The path followed along the fixed-point branches is not identical whether the control parameter increases or decreases. As it discriminates between increasing and decreasing values, the system seems to “remember” former values of transglutaminase activity.

The shape of the bifurcation diagram depends on the other parameter values. Of interest is the dependence of the  $k_g g$  threshold on  $K_G$  values. As shown in Fig. 6, the transglutaminase concentration necessary to switch from the “low-matrix” to the “high-matrix” branch increases

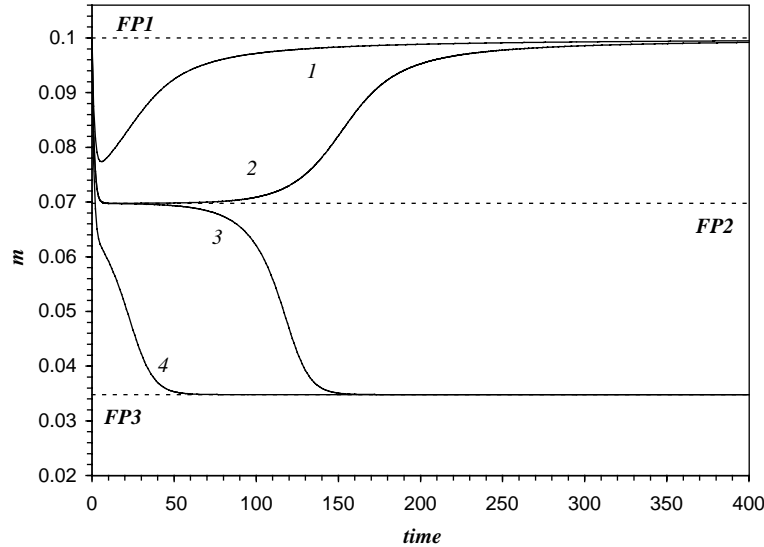


FIG. 4. Bistability and sensibility to perturbations. For each curve, initial ECM proteins concentration is maximal  $m(0) = c_0$ , and initial proteinase concentration  $p(0)$  is 0.2 (curve 1), 0.2875 (curve 2), 0.2876 (curve 3) and 0.40 (curve 4). Equation (3) is then integrated numerically with  $k_{gg} = 0.05$ , and all other parameters as in Fig. 3. The  $m$  component values of the three fixed points are indicated (dashed lines).

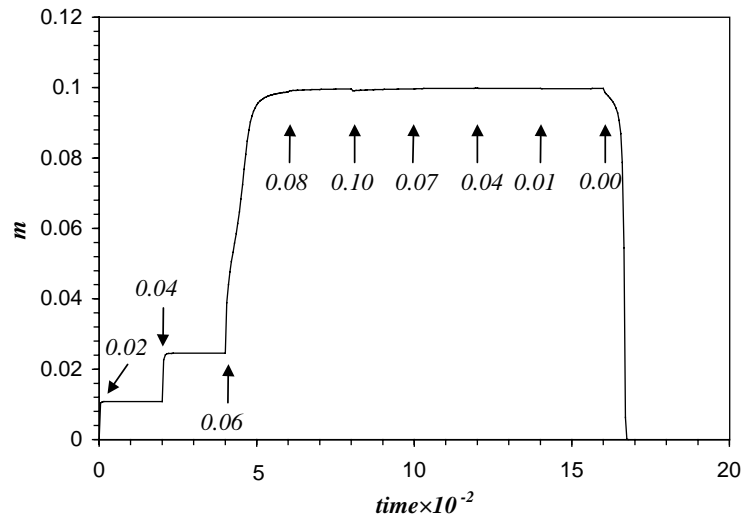


FIG. 5. Hysteresis (memory) behavior of the closed model [eqn (3)] exemplified by ECM proteins evolution  $[m(t)]$  with varying transglutaminase activities. Numerical integration is initiated with initial conditions:  $m(0) = 0$ ,  $p(0) = 1.0$  and  $k_{gg} = 0.02$ . At indicated times (arrows),  $k_{gg}$  is modified as shown beneath the arrows. All other parameters are kept constant and are those of Fig. 3.

linearly with decreasing enzyme affinity, which is in agreement with intuitive expectations. Likewise, the shape of the FP2 and FP3 branches and the distance between the saddle-node bifurcation and FP1 depend on the parameters. An extreme example with low  $K_R$  ( $K_R = 0.001$ ) is presented in Fig. 7. Whereas the bifurcation diagram for  $p$

resembles those obtained with higher  $K_R$  [cf. Figs 3 and 7(A)], the  $m$  diagram [Fig. 7(B)] is qualitatively different: the low (FP3) stable branch exhibits a hyperbolic shape which rapidly tends to FP1 [Fig. 7(B)]. The unstable branch (FP2) cannot even be distinguished in this figure. These characteristics have interesting

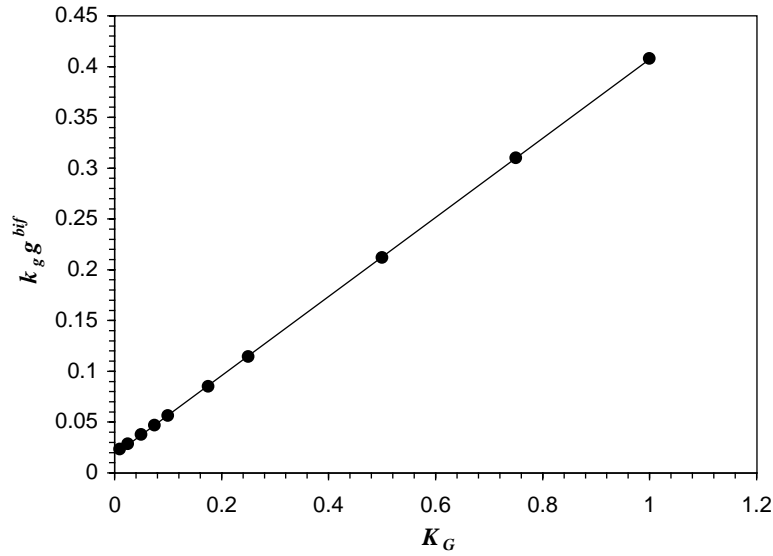


FIG. 6. Dependence on transglutaminase affinity ( $K_G$ ) of the transglutaminase activity at the FP2–FP3 saddle-node bifurcation ( $k_g g^{bif}$ ). All parameters (except  $K_G$ ) are the same as Fig. 3.

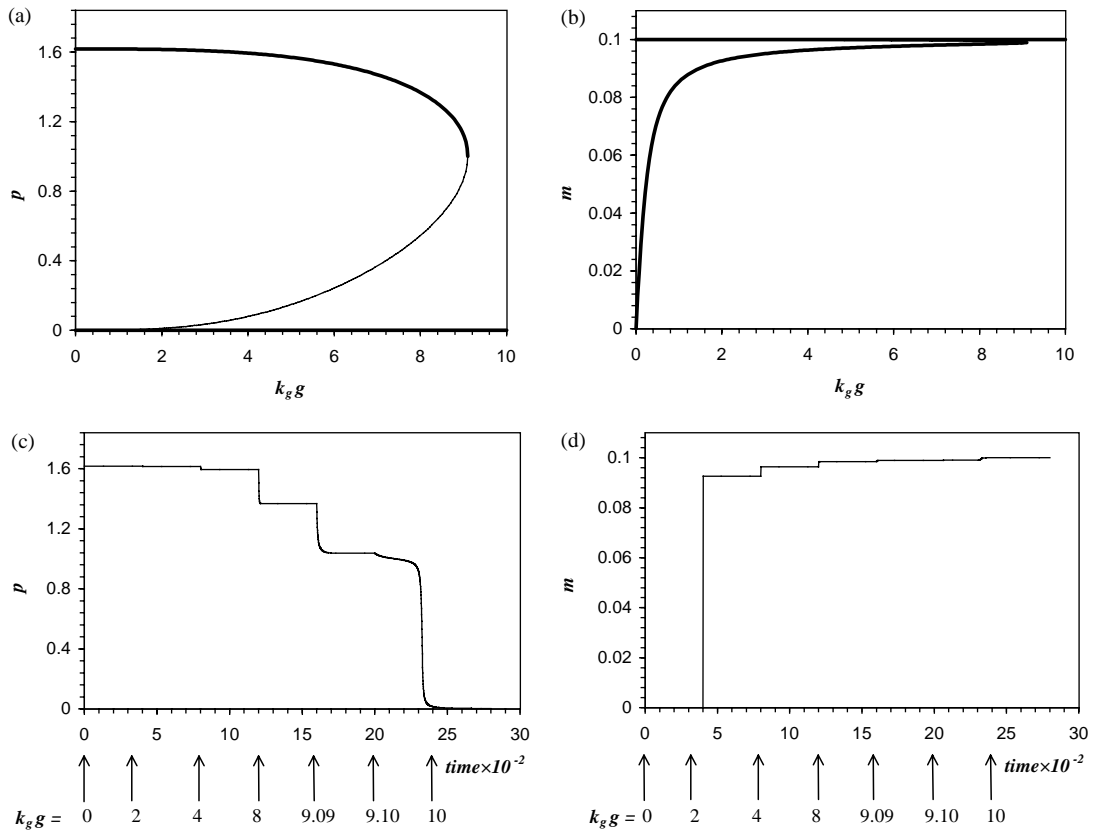


FIG. 7. Closed model with low  $K_R$  value. (a, b) Bifurcation diagrams for  $p$  (a) and  $m$  (b) with transglutaminase activity ( $k_g g$ ) as the control parameter. Bold lines represent stable fixed points and thick lines unstable ones. (c, d) Paths along the branches for  $p(t)$  (c) and  $m(t)$  (d). Numerical integration initiated with  $m(0) = 0$ ,  $p(0) = 1.618$  and no transglutaminase ( $k_g g = 0$ ). Every 400 time units (arrows),  $k_g g$  is increased to the value indicated. Parameters are:  $K_R = 0.001$ ;  $K_G = 0.1$ ;  $K_{deg} = k_{deg} = 1$ ;  $n = 3$ ;  $\alpha = 1$ ;  $c_0 = 0.1$  and  $r_{im} = \delta = 0$ .

consequences on the evolution of  $p$  and  $m$  with variable transglutaminase activities. In the absence of transglutaminase ( $k_{gg} = 0$ ) and without initial ECM, the model is in the “low-matrix” fixed point FP3 [Fig. 7(C) and (D),  $t = 0$ ]. As  $k_{gg}$  increases,  $m$  first abruptly increases, then hardly varies. This “switch-like” behavior is caused by the sharp increase of the FP3 branch, but does not correspond to a branch switch in the bifurcation diagram. Consistently,  $p$  remains largely unchanged while  $k_{gg} < 8$ , because its FP3 branch [(Fig. 7A)] is almost constant. Hence for intermediate transglutaminase activities (i.e.  $2 < k_{gg} < 8$ ), the system auto-organizes into a state with high ECM concentrations (and low fragment) together with high proteinase levels. Further  $k_{gg}$  increase causes the system to switch from FP3 to FP1 when the bifurcation point is exceeded. Whereas the influence on  $p$  is notable [Fig. 7(C),  $t > 2000$ ], it can barely be observed on  $m$  because the  $m$  values of FP3 and FP1 at the bifurcation are very similar. Thus,  $m$  and  $p$  seem to become uncoupled:  $m$  seems to switch a fixed point for low transglutaminase activities, whereas  $p$  switches for substantially higher values. The paradoxical result that a stable steady state can be obtained where both proteinase and ECM concentrations are high can be explained on the basis of the  $K_R$  value which is very low in Fig. 7. In this case, proteinases are highly expressed, even with low fragment (or equivalently high ECM) concentrations. This situation is stable as far as transglutaminase activity is high enough to maintain elevated ECM concentrations but the corresponding low fragment concentration is still high enough to maintain elevated levels of proteinase neo-synthesis.

### 5. “Open” Model

With non-zero values for  $r_{im}$  and  $\delta$ , eqn (2) describes an “open” model in which the total (ECM proteins + proteolysis fragments) concentration is not conserved. Numerical integration of eqn (2) shows that the behavior of the system is then drastically modified. Sustained oscillations of the three variables, reflecting the emergence of a stable limit cycle (Fig. 8), appear. When  $f < K_R$  [0.2 in Fig. 8(A) and (B), 0.01 in

Fig. 8(C) and (D)],  $p$  decreases because of autoproteolysis. The limit cycle being clockwise [Fig. 8(B) and (D)], this comes with an increase in  $m$  owing to constant ECM input (the system runs along the lower part of the limit cycle). Under the action of the residual proteinases on  $m$ ,  $f$  increases when ECM concentration becomes elevated. The upper-left corner of the limit cycle (in the  $m$ - $p$  space) is reached when fragment concentration crosses over  $K_R$ . Then  $p$  abruptly increases because of fragment-induced neo-synthesis: the system runs along the upper part of the limit cycle of Fig. 8. Proteinase substrate (ECM proteins and fragments) concentration consequently abruptly decreases and another cycle begins.

As exemplified in Fig. 8, a variety of characteristics (shape, amplitude, phase) can be observed with the oscillation’s period varying between 10 and  $5 \times 10^2$  time units (Fig. 9). Figure 10 presents a bifurcation diagram with transglutaminase activity as the control parameter. For low  $k_{gg}$ , a single fixed point exists and is stable. With increasing transglutaminase activity, the system crosses over a Hopf bifurcation: the former stable fixed point becomes unstable and a stable limit cycle appears. As  $k_{gg}$  further increases, the stable limit cycle fuses with an unstable one, forms a semi-stable limit cycle at the bifurcation (SSLC: a limit cycle with stable interior and unstable exterior) and disappears.

A simplifying biological interpretation of this phase diagram would consist in assigning each of its regions to a biological state of the ECM. An important outcome is that, as seen in the bifurcation diagrams, this “open” version of the model does not show a stable state with high ECM and low proteinase concentrations, which would *a priori* be considered as a normal physiological condition. For transglutaminase activities lower than the Hopf bifurcation, the system presents a stable steady state but in this state, the ECM density is low and the proteinase concentration is high. This would be a favorable state for tumor development and dissemination, for instance. On the other hand, high transglutaminase activities (above the SSLC bifurcation) correspond to unstable regions which yield high ECM and low proteinase concentrations. But

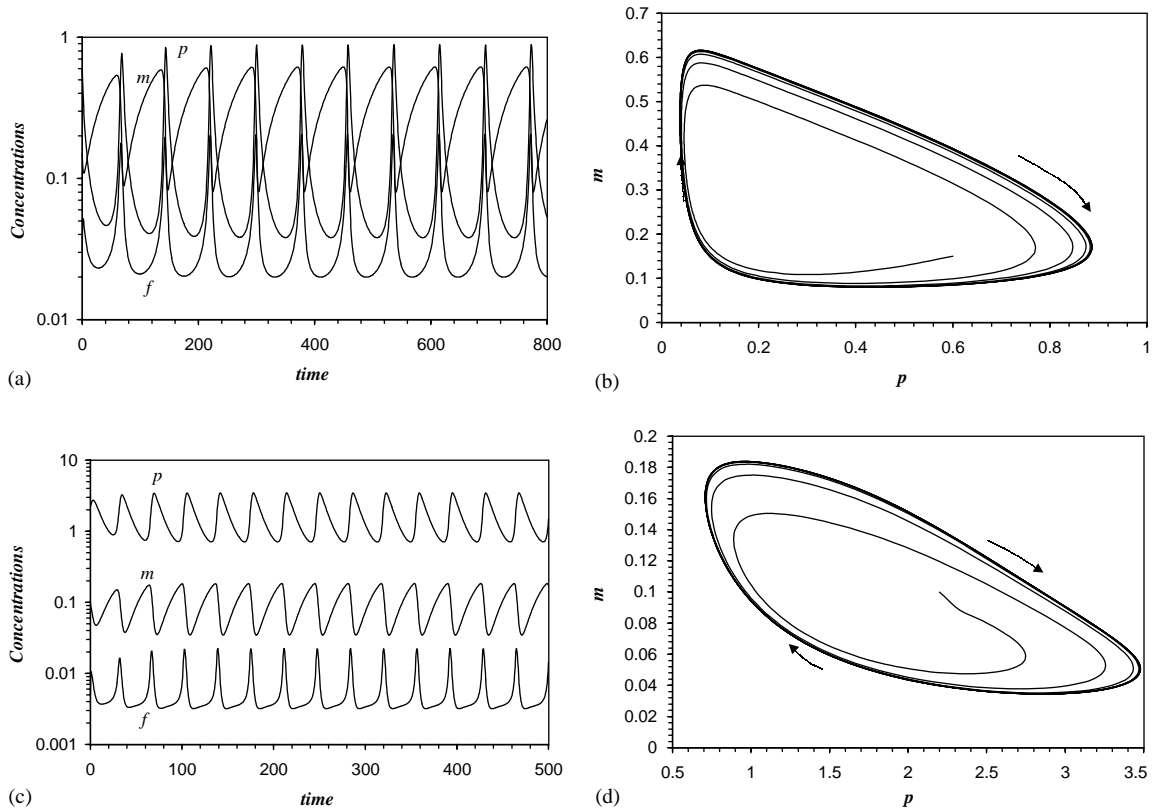


FIG. 8. Sustained oscillations displayed by the “open” model [eqn (2)] for various parameter sets. (a, c) temporal variations of the three concentrations  $p$ ,  $m$  and  $f$ . (b, d) Projections in the  $(m-p)$  plane of the corresponding limit cycles. Both cycles are clockwise (arrows). Parameters are:  $K_R = 0.2$ ;  $K_G = 0.1$ ;  $K_{deg} = k_{deg} = 1$ ;  $k_{gg} = 0.05$ ;  $n = 3$ ;  $\alpha = 1$ ;  $r_{im} = 0.01$  and  $\delta = 1$  (a, b);  $K_R = K_G = K_{deg} = 0.01$ ;  $k_{deg} = 0.1$ ;  $k_{gg} = 0.32$ ;  $n = 3$ ;  $\alpha = 1$ ;  $r_{im} = 0.01$  and  $\delta = 1$  (c, d).

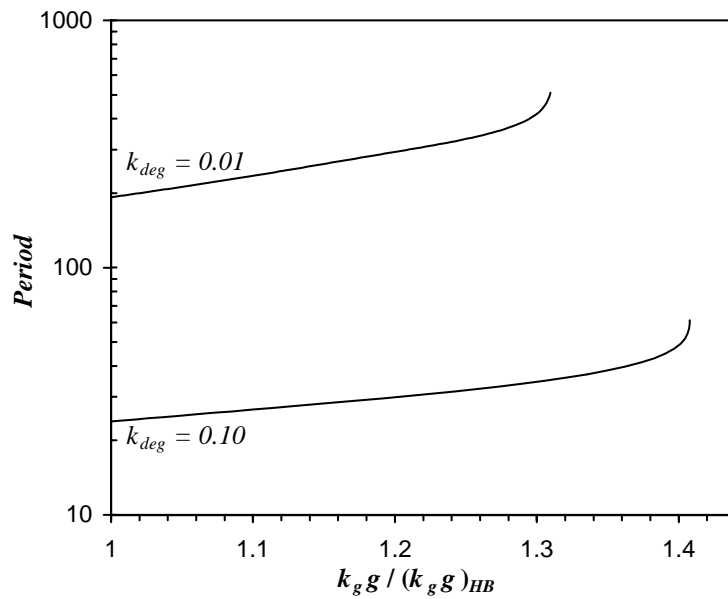


FIG. 9. Oscillation period as a function of the relative transglutaminase activity  $k_g g / (k_g g)_{HB}$  with two different autoproteolytic activities  $k_{deg}$ .  $(k_g g)_{HB}$  stands for the  $k_g g$  value at the Hopf bifurcation for the considered parameter set:  $(k_g g)_{HB} = 3.349$  with  $k_{deg} = 0.01$  and  $(k_g g)_{HB} = 0.241$  with  $k_{deg} = 0.10$ . Parameters are:  $K_R = K_G = K_{deg} = 0.01$ ;  $k_{deg} = 0.1$ ;  $n = 3$ ;  $\alpha = 1$ ;  $r_{im} = 0.01$  and  $\delta = 1$ .

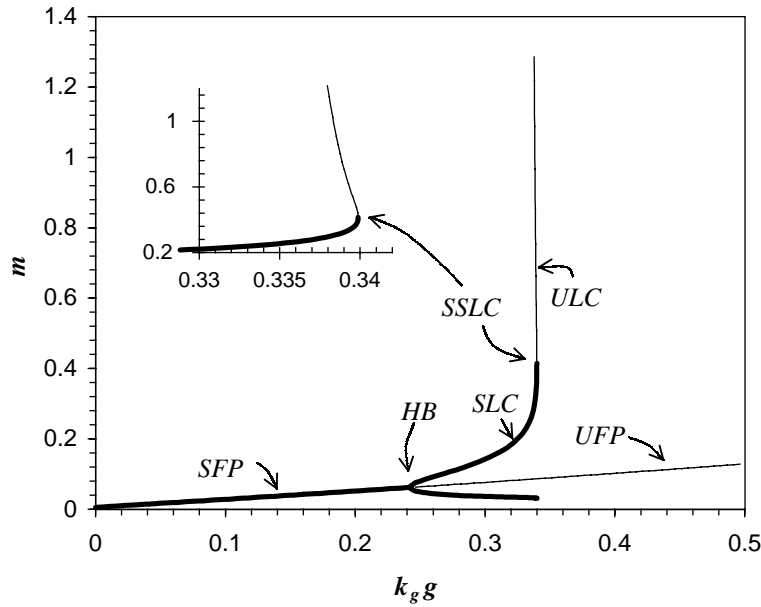


FIG. 10. Bifurcation diagram for  $m$  [“open” model, eqn (2)] with  $k_g g$  (transglutaminase activity) as the control parameter. Bold lines represent stable fixed points or limit cycles, thin lines are unstable ones. Only the envelopes (minimal and maximal values) of the limit cycles are presented. As the parameter increases, a stable fixed point (SFP) changes to an unstable fixed point (UFP) through a Hopf bifurcation (HB), i.e. the emergence of a stable limit cycle (SLC). The latter disappears after fusion with an unstable limit cycle (ULC), in a semi-stable limit cycle (SSLC) bifurcation. The inset is an enlargement of the SSLC bifurcation zone. Parameters are:  $K_R = K_G = K_{deg} = 0.01$ ;  $k_{deg} = 0.1$ ;  $n = 3$ ;  $\alpha = 1$ ;  $r_{im} = 0.01$  and  $\delta = 1$ .

this steady state is unstable so that ECM concentration increases unboundedly and proteinase concentration vanishes with time. This could correspond to known pathologies, such as fibrosis where ECM is overabundant and, more importantly, grows out of control.

Thus one possible interpretation, although speculative, is that the normal physiological state could correspond to the oscillatory domain, where the average ECM concentration is constant and relatively high. Oscillation periods vary between 10 and  $5 \times 10^2$  non-dimensional ( $1/k_p$ ) time units (Fig. 9). With  $k_p$  varying from 50 to  $500 \text{ hr}^{-1}$  (see Section 2), this yields a period interval ranging, in natural units, from seconds to minutes. This could be too small to be detected by conventional experimental techniques in cellular biology, that would only exhibit an average, constant ECM level. Interestingly, in this interpretation, homeostasis of ECM remodeling thus results from an oscillating mechanism, providing a seemingly constant average level.

Proteinase autoproteolysis is an important parameter for the structure of the bifurcation

diagram. Figure 9 shows that oscillation period increases with decreasing  $k_{deg}$ . Furthermore, the distance between the Hopf and SSLC bifurcations decreases with increasing  $k_{deg}$  (Fig. 11). Eventually, this distance vanishes [Fig. 11(B)] and the Hopf bifurcation directly gives rise to the unstable limit cycle (the stable limit cycle disappears). Thus high proteinase autoproteolysis suppresses the sustained oscillations.

The dependence on the other parameters is presented with two-parameter stability diagrams in Fig. 12. Before more detailed interpretations, it can be remarked that in all cases, the oscillatory zone is narrow. Note that in Fig. 12, the stability diagrams are presented in log-log coordinates for clarity so that the width of the oscillatory zones appears even thinner than in natural coordinates. Rapid estimations indicate that, if located in the middle of an oscillatory zone, the minimal parameter variation required to leave the zone lies on average between 10 and 40%. We think that these values are higher than naturally occurring noise-induced parameter variability in biological systems. However, these

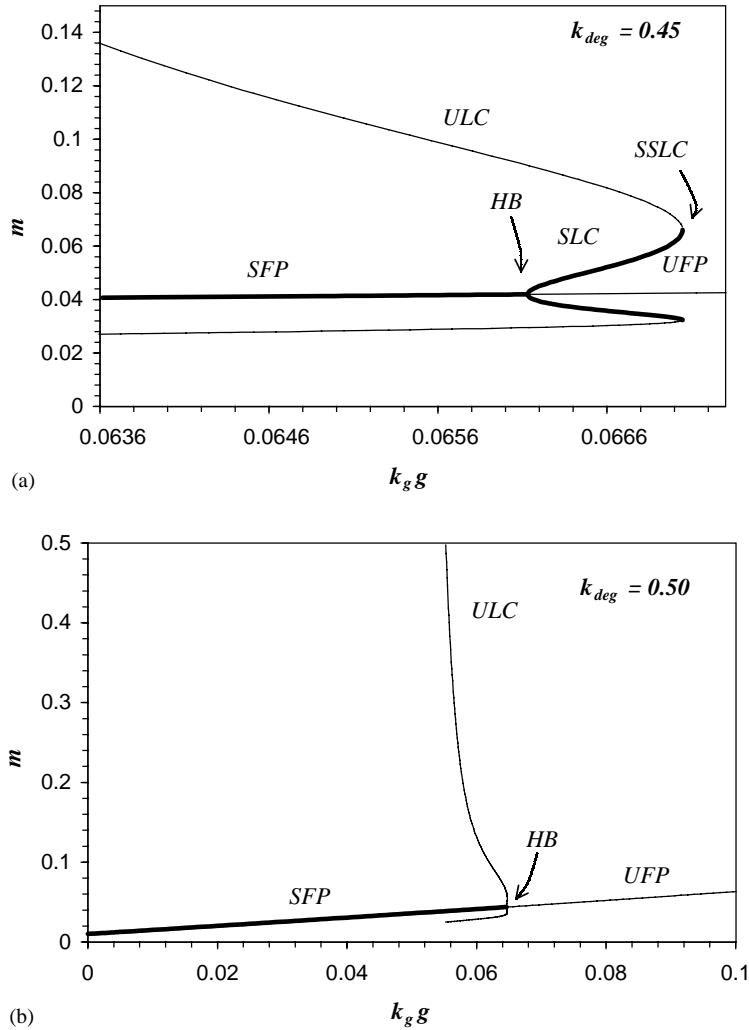


FIG. 11. Sustained oscillations depend on proteinase autoproteolysis. Bifurcation diagrams for two values of  $k_{deg}$  [eqn (2)]:  $k_{deg} = 0.45$  (a) or  $0.50$  (b). All other parameters and figure legends are as Fig. 9.

low values indicate that the system should be tightly regulated in order to maintain oscillatory properties.

Figure 12(A) summarizes the preceding remarks. With increasing  $k_g g$ , and constant  $k_{deg}$ , the system goes by Hopf bifurcation and displays sustained oscillations for  $k_{deg} < 0.5$ . Furthermore, oscillations develop at lower proteinase autoproteolysis if transglutaminase activity is increased. As mentioned above, oscillations develop when  $p$  can decrease by autoproteolysis during a phase of the cycle. This is possible only if  $f$  remains less than  $K_R$  during this phase, i.e. if transglutaminase activity is sufficient to decrease fragment concentration to lower values. With high transglutaminase

activities, the  $K_R$  threshold is less easily reached, so that the requirement for high autoproteolysis to decrease  $p$  is less drastic. In fact, if transglutaminase concentration  $g$  is an adjustable parameter, oscillations can accommodate up to circa two orders of magnitude of  $k_{deg}$  variation.

The other stability diagrams, however, show that locating into stability/oscillation areas can also be controlled by virtually all the other parameters. Figure 12(B) shows that sustained oscillations can be triggered by high values of the maximal cell response to fragments ( $\alpha > 1$ ). Modulation of signal transduction pathways can thus regulate the oscillatory behavior of the system. Moreover, Fig. 12(B) indicates that if

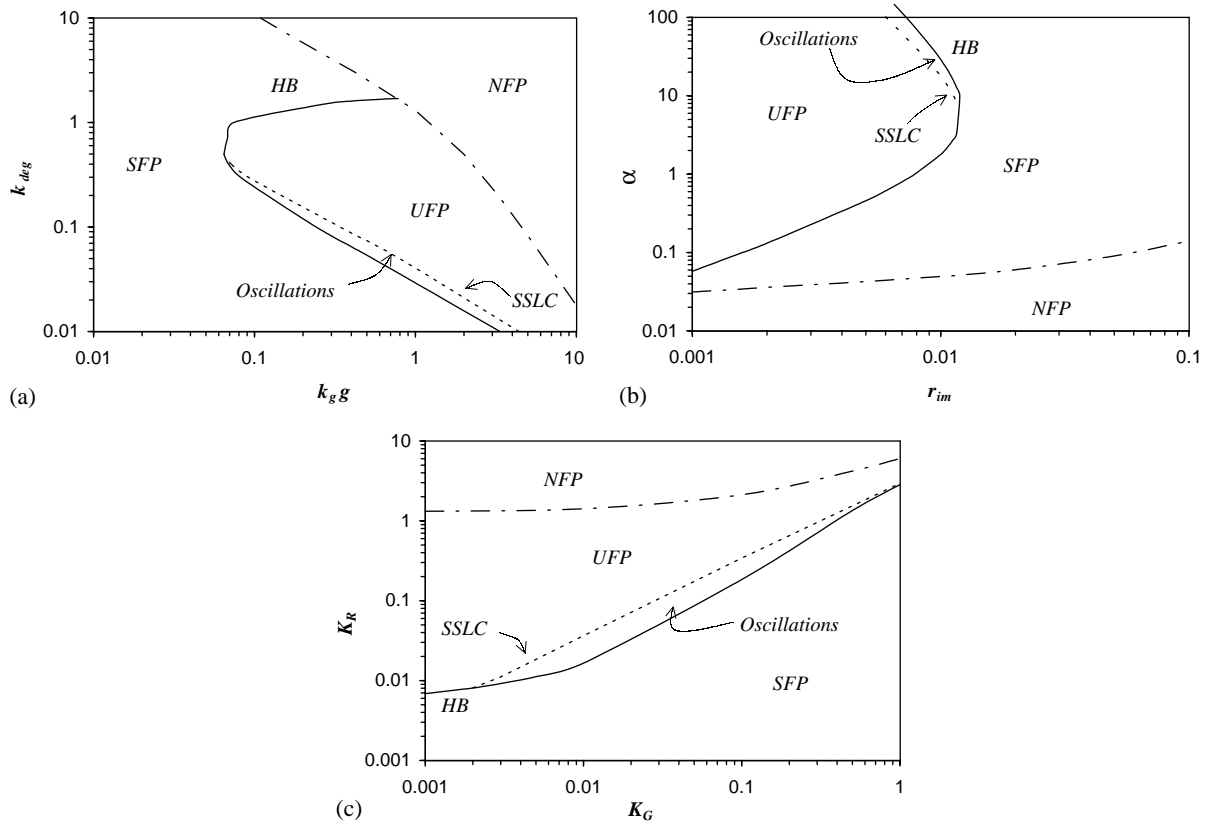


FIG. 12. Two-parameters stability diagrams. Oscillations arise in zones delineated by a Hopf bifurcation (HB, full lines) and a semi-stable limite cycle (SSLC, dashed lines) bifurcation. SFP: stable fixed point; UFP: unstable fixed point; NFP: no fixed point. Parameters are:  $K_R = K_G = K_{deg} = 0.01$ ;  $n = 3$ ;  $\alpha = 1$ ;  $r_{im} = 0.01$  and  $\delta = 1$ (a);  $K_R = K_G = K_{deg} = 0.01$ ;  $k_{deg} = 1$ ;  $k_{gg} = 0.05$ ;  $n = 3$  and  $\delta = 1$ (b);  $K_{deg} = k_{deg} = 1$ ;  $k_{gg} = 0.05$ ;  $n = 3$ ;  $\alpha = 1$ ;  $r_{im} = 0.01$  and  $\delta = 1$  (c).

ECM production rate ( $r_{im}$ ) is decreased, oscillations can be preserved by increasing  $\alpha$ . This is a result of the complex dynamics of eqn (2).

Figure 12(C) presents the system's behavior as a function of transglutaminase's affinity ( $K_G$ ) and the sensibility of the cell response to fragments ( $K_R$ ). Clearly, if one of these parameters is adjustable, oscillations can develop over two orders of magnitude of both parameter variations. If transglutaminase affinity is highly decreased, oscillations can be maintained by decreasing the cell maximal response to fragments, or conversely, increasing the fragment concentration threshold that is necessary to trigger a high proteinase expression level. However, Fig. 12(C) indicates that oscillations arise for low  $K_G$  values, i.e. if transglutaminase affinity for its substrate  $f$  is greater than proteinase affinity for  $m$ . This is actually the case *in vivo* (see Section 3). Finally, we notice in this figure that for constant  $K_G$  values, oscilla-

tions and stability properties of eqn (2) can be regulated by modulating  $K_R$ . The first molecular event involved in proteinase transduction pathways is the fragment recognition by the cellular receptor. Undoubtedly, the affinity of the receptor for the fragment would influence the value of  $K_R$ . In the case of the integrin family of receptors, the cells can modify the affinity of their receptors for their ECM ligands, in a process termed "inside-out" signaling (Yamada, 1997; Bouvard *et al.*, 1998). Consequently, inside-out signaling is an example of how cells could regulate their positioning in the stability diagrams and switch from the low-ECM invasive state to the oscillatory homeostatic one.

## 6. Discussion

A large amount of work has been dedicated in the past years to the modeling of extracellular

matrix degradation and its relations with invasive cells (Perumpanani *et al.*, 1996, 1998; 1999; Perumpanani & Byrne, 1999; Landmann & Pettet, 1998; Berry & Larreta-Garde, 1999; Dallon *et al.*, 1999; Webb *et al.*, 1999). In these studies, the ECM mass balance primarily depends on the catabolic action of proteinases and ECM production by the cells. Our main objective in this article consisted in the introduction of transglutaminases in such a model. As these widespread enzymes can turn soluble proteins into insoluble lattices, their influence on the mechanical properties of the ECM appears to be the reverse of the action of proteinases. We thus treated proteinases and transglutaminases as reverse catalysts of a futile cycle in which ECM proteins and their soluble proteolysis fragments are interconverted. Furthermore, our model implicitly assumes that proteinase expression is regulated by the quantity of soluble ECM proteolysis fragments and not by the quantity of native ECM proteins, i.e. that outside-in cell signaling in response to cell-ECM interactions varies with the physical state of the ECM proteins. This assumption is first based on experimental evidences that the regulation of cell migration (Gianelli *et al.*, 1997) or proteinase expression (Werb *et al.*, 1989) is mediated by ECM proteolysis fragments but not by the corresponding entire proteins. Further, it relies on growing amount of reports that the mechanical and physical characteristics of the ECM, such as rigidity or elasticity, can by themselves regulate cell physiology, irrespective of the chemical identity of the proteins the ECM contains (Choquet *et al.*, 1997; Hynes, 1999; Katz *et al.*, 2000).

The structure of our model can thus be described as a cyclic bienzymatic system, with a positive-feedback regulation. Several models of cyclically organized biological reaction have previously been studied. In the absence of regulation, the only dynamical behavior accessible is monostability, although switch-like properties can be observed through zero-order ultrasensitivity (Goldbeter & Koshland, 1982; Ferrell, 1996; Ferrell & Machleder, 1998). When self-regulation is included, bistability may be obtained (Lisman, 1985; Hervagault & Canu, 1987; Thron, 1999; Zhabotinsky, 2000; Ferrell &

Xiong, 2001), as well as more complex dynamics if several bienzymatic cycles are themselves organized in a cyclic fashion (Gonze & Goldbeter, 2000). Many of the theoretical predictions of these models have been confirmed experimentally (Schellenberger & Hervagault, 1991; Coevoet & Hervagault, 1997; Guidi & Goldbeter, 1998). *In vivo*, however, few enzyme categories are known to form bienzymatic cycles. The main but ubiquitous example concerns enzymes involved in phosphorylation/dephosphorylation events. Thus most of the previously published studies of bienzymatic cycles relate to kinase/phosphatase cycles although others have been proposed, including isocitrate dehydrogenase/diaphorase (Guidi & Goldbeter, 1998, 2000). Seen from this angle, our model introduces a new category of enzyme families possibly involved in a bienzymatic cycle: the proteinase/transglutaminase activities. Note, however, that transglutaminase activity could be generalized to other enzymes, such as protein disulfide isomerases or more generally, protein cross-linking enzymes.

Indeed, the equation describing the model [eqn (2)] exhibits bistability if ECM production by the cells and ECM fragments proteolysis are neglected. Fundamentally, the system possesses two states for the ECM proteins: a low-concentration one and a high-concentration one. These two states respectively correspond to a high proteinase concentration state and a low proteinase concentration one. The dynamics consist in switches between these two states including memory and threshold properties. Under physiological conditions, the ECM is a physical barrier to cell displacement. To disseminate and form distant metastases, invasive cells counteract this barrier by the production of extracellular proteinases that locally degrade the ECM and render it porous to the cells (Heino, 1996; Price *et al.*, 1997). Thus, the low-ECM/high-proteinase state of eqn (2) can be interpreted as prone to metastasis dissemination. Accordingly, the engagement of non-invasive cancer cells into the invasive aggressive phenotype could be interpreted as a switch toward the low-ECM/high-proteinase state. To this end, proteinase production and secretion by the cells would not be sufficient. The switch would be

effective only if proteinase concentration gets higher than a threshold that depends on the cell and its ECM properties. This could explain that proteinase production in the ECM is not always a hallmark of invasive cells by itself, inasmuch as some normal healthy cells produce proteinases to locally control the ECM (Duffy & McCarthy, 1998; Murphy & Gavrilovic, 1999). The usual point of view is that cell invasion would be brought about by proteinase overload (Liotta *et al.*, 1991; Cockett *et al.*, 1998), which is in agreement with the threshold properties of our model. Conversely, this would indicate that treatments with proteinase inhibitors to prevent malignant invasion would be efficient only if they decrease proteinase levels below the threshold. This could, together with other factors (McCawley & Matrisian, 2001) account for the disappointing results of some of the synthetic inhibitors which are in later stages of clinical trials (Duffy & McCarthy, 1998; McCawley & Matrisian, 2000). Furthermore, the possibility to highly distort the bistable bifurcation diagram with varying parameters enables some biological interpretations which would be difficult to obtain with a classical “S-shaped” diagram. In the case of Fig. 7, for instance, this allows an apparent uncoupling of the two variables in the diagram. Additionally, a parameter zone can be observed where the high transglutaminase activity compensates the high proteinase level, allowing coexistence of high ECM concentrations with high proteinase concentrations.

In a model for the isocitrate dehydrogenase reaction, Guidi & Goldbeter (1998, 2000) have shown that the batch bistable version of the model may become oscillatory when the system is opened to constant reactant influx and efflux. We observed the same transition from bistability to oscillations when constant ECM production by the cells and fragment degradation are included in our model (Fig. 8). Bifurcation and stability diagrams (Figs 10–12) roughly present three main zones that can be ascribed to different biological situations. Stability areas contain stable fixed points that, in most cases, are low-ECM/high-proteinase states. This could be a picture of the situation encountered during cell invasion. Unstable zones include areas characterized by unstable fixed points only or

absence of any attracting items. In most of these cases, the proteinase and fragment concentrations rapidly vanish with time so that ECM quantity grows unboundedly. One can think of these areas as reflecting pathologies like fibrosis arising from uncontrolled ECM growth.

Finally, oscillation areas, bounded by the Hopf and semi-stable limit cycle bifurcations, could be assimilated to the normal physiological situation. The originality of this interpretation lies in the conception of the ECM mass balance as a homeostatic oscillator. Considering the narrowness of the oscillation areas, this view however implies a tight regulation by the system. Indeed, positioning into the stability diagram can be controlled by most of the model parameters (Fig. 12). The transition from the low-ECM “invasive” state to the normal homeostatic oscillatory regime could then be elicited by the cell itself via increases in transglutaminase quantity ( $k_{gg}$ ), variations in the ECM production rate ( $r_{im}$ ), quantitative modifications of the transduction pathways leading to proteinase expression ( $\alpha$ ) or inside-out signaling (cell-controlled changes in ECM receptor affinity). The model therefore appears to reflect well the multi-controlled and complex system formed by the cells and the ECM.

In both the “open” and the “closed” models, the value of the Hill coefficient  $n$  is an important parameter. The “closed” model presents three steady states for  $n \geq 2$ . However, in the case  $n = 2$ , the degenerate node (FP1) is hardly stable, even for high  $k_{gg}$  values (not shown). The model is thus bistable for  $n \geq 3$ . With increasing  $n$  values, the second saddle-node bifurcation (FP2–FP3 branch fusion) occurs at decreasing values of the control parameter  $k_{gg}$ . The “open” model also shows Hopf bifurcation and sustained oscillations for  $n \geq 2$ . With increasing  $n$  values, the behavior is qualitatively conserved, but the Hopf bifurcation occurs at lower values of the control parameter  $k_{gg}$  (not shown). Thus, the  $n$  value used in this article ( $n = 3$ ) is a minimal value for the two models and seems compatible with even mildly cooperative systems *in vivo*.

In this work, proteinase autoproteolysis has been modeled with a Michaelis-type expression. This is a crude approximation because

Michaelis–Menten kinetics rigorously hold for high initial substrate-to-enzyme concentration ratios. This restriction is not obvious when both enzyme and substrates are the same molecular species. Other kinetic expressions can be thought of. For instance, a sigmoid expression could be used to express the autocatalytic nature of autoproteolysis. We have checked that the dynamical behaviors described in this paper do not qualitatively change if the autocatalytic term [second term in the right-hand side of eqn (1c)] is replaced by a Hill function of the form  $-ap^q/(K^q + p^q)$ , where  $q$  is the corresponding Hill number. With this modification, the “closed” model still presents bistability, although for different parameter values, if  $n$  and  $q$  are  $\geq 1$ , and whatever the  $n$  value with respect to  $q$ . The “open” model also still shows sustained oscillation zones after this modification, whenever  $n \geq 2$  and  $q \geq 1$ . In this case, the value of the control parameter  $k_{cg}$  at the Hopf bifurcation increases with increasing  $q$  values.

Other expressions for the autocatalytic term are conceivable. Actually, the main basic requirement for this term is the need for a possible proteinase output from the system, which excludes systematic  $p$  unlimited growth due to neo-synthesis. This can therefore be interpreted as autoproteolysis, irreversible inhibition (mediated by  $\alpha$ -macroglobulin, for example; see Birkedal-Hansen *et al.*, 1993), or simply uptake by the biological surroundings. For instance, in some models for tumor growth, proteinase decay has been modeled by first-order kinetics (Perumpanani *et al.*, 1996, 1998; Perumpanani & Byrne, 1999). For the “closed” model, changing the autocatalytic term to first-order kinetics alters the shape of the nullcline for  $dp/dt$  to a sigmoid shape (Fig. 2), but does not suppress the occurrence of bistability. The qualitative behavior is thus conserved. On the other hand, the Michaelis–Menten expression used for autoproteolysis in eqn (1c) reduces to such first-order kinetics when the proteinase concentration is much higher than  $K_{deg}$ . Now, in the results presented in Fig. 8(C) for the “open” model,  $p$  is always much greater than  $K_{deg}$  so that our autoproteolysis kinetics can really be considered here as first order throughout the oscillatory cycle. Taken

together, these observations indicate that the origination of sustained oscillations or bistability is not critically dependent on the exact nature of the mathematical expression used to model proteinase output from the system.

Experimental examination of these predictions could be difficult to achieve because the oscillation periods could be too small to be detected by conventional cell-culture techniques. A suitable experimental method should record local proteinase, fragment or ECM protein kinetics among cell cultures in *continuous* mode. In principle, this could be achieved by monitoring fluorescent (*gfp*-tagged) proteinases, for instance. This technique has been used to study fibronectin dynamics inside cell-culture-derived ECM (Ohashi *et al.*, 1999). Fibronectin is a large ECM glycoprotein ( $\approx 500$  kDa) so that it can safely be assumed that its properties are not dramatically modified by *gfp* labeling. This could be less obvious with ECM proteinases, that are much smaller ( $\approx 60$ – $70$  kDa) and must maintain catalytic activity in the presence of the fluorescent tag. Alternatively, proteinase activity could be continuously monitored by incorporating low quantities of exogenous proteolysis markers into the ECM. This approach has been successfully achieved using a chemically modified bovin serum albumin that becomes fluorescent upon proteolysis and has evidenced that pericellular ECM proteolysis during neutrophil migration is oscillatory, with periods of the order of 20 s (Kindzelskii *et al.*, 1998). The oscillation periods accessible to this kind of experiment are thus compatible with those predicted in the present paper.

Finally, many of the *in vivo* interactions are neglected in our model, especially as far as transglutaminase regulation is concerned. For instance, transglutaminase is known to undergo deactivation by proteolysis (Belkin *et al.*, 2001). Furthermore, transglutaminase expression and secretion by the cells can be regulated by the quantity of surrounding ECM (Haroon *et al.*, 1999). We are currently studying a modified version of eqn (2) that takes this feature into account. Preliminary results show that this model exhibits complex transitions to chaos for some parameter values. Hence, including transglutaminase action in simple models for ECM

degradation balance yields enriched dynamics that could be better suited to model this complex biological system.

We wish to thank Prof. N. Lomri, ERRMECe, Université de Cergy-Pontoise, France, for the critical reading of the manuscript.

## REFERENCES

- AESCHLIMANN, D. & THOMAZY, V. (2000). Protein cross-linking in assembly and remodelling of extracellular matrices: the role of transglutaminases. *Connect. Tissue Res.* **41**, 1–27.
- AKIMOV, S. S. & BELKIN, A. M. (2001). Cell surface tissue transglutaminase is involved in adhesion and migration of monocyte cells on fibronectin. *Blood* **98**, 1567–1576.
- ATKINSON, S. J., CRABBE, T., COWELL, S., WARD, R. V., BUTLER, M. J., SATO, H., SEIKI, M., REYNOLDS, J. J. & MURPHY, G. (1995). Intermolecular autolytic cleavage can contribute to the activation of progelatinase A by cell membranes. *J. Biol. Chem.* **270**, 30 479–30 485.
- BAGOWSKI, C. P. & FERRELL, J. E. (2001). Bistability in the JNK cascade. *Curr. Biol.* **11**, 1176–1182.
- BASBAUM, C. B. & WERB, Z. (1996). Focalized proteolysis: spatial and temporal regulation of extracellular matrix degradation at the cell surface. *Curr. Opin. Cell Biol.* **8**, 731–738.
- BELKIN, A. M., AKIMOV, S. S., ZARITSKAYA, L. S., RATNIKOV, B. I., DERYUGINA, E. I. & STRONGIN, A. Y. (2001). Matrix-dependent proteolysis of surface transglutaminase by membrane-type metalloproteinase regulates cancer cell adhesion and locomotion. *J. Biol. Chem.* **276**, 18 415–18 422.
- BERRY, H. & LARRETA-GARDE, V. (1999). Oscillatory behavior of a simple kinetic model for proteolysis during cell invasion. *Biophys. J.* **77**, 655–665.
- BERRY, H., PELTA, J., LAIREZ, D. & LARRETA-GARDE, V. (2000). Gel–sol transition can describe the proteolysis of extracellular matrix gels. *Biochim. Biophys. Acta* **1524**, 110–117.
- BIRKEDAL-HANSEN, H., MOORE, W. G. I., BODDEN, M. K., WINDSOR, L. J., BIRKEDAL-HANSEN, B., DECARLO, A. & ENGLE, J. A. (1993). Matrix metalloproteinases: a review. *Crit. Rev. Oral Biol.* **4**, 197–250.
- BOUVARD, D., MOLLA, A. & BLOCK, M. R. (1998). Calcium/calmodulin-dependant protein kinase II controls  $\alpha 5\beta 1$  integrin-mediated inside-out signaling. *J. Cell Sci.* **111**, 657–665.
- CHOQUET, D., FELSENFELD, D. P. & SHEETZ, M. (1997). Extracellular matrix rigidity causes strengthening of integrin–cytoskeleton linkages. *Cell* **88**, 39–48.
- CHUNG, S. I., SHRAGER, R. I. & FOLK, J. E. (1970). Mechanism of action of guinea pig liver transglutaminase VII—chemical and stereochemical aspects of substrate binding and catalysis. *J. Biol. Chem.* **245**, 6424–6435.
- COCKETT, M. I., MURPHY, G., BIRCH, M. L., O'CONNELL, J. P., CRABBE, T., MILLICAN, A. T., HART, I. R. & DOCHERTY, A. J. P. (1998). Matrix metalloproteinases and metastatic cancer. *Biochem. Soc. Symp.* **63**, 295–313.
- COEVOET, M.-A. & HERVAGULT, J.-F. (1997). Irreversible metabolic transitions: the glucose 6-phosphate metabolism in yeast cell-free extracts. *Biochem. Biophys. Res. Commun.* **234**, 162–166.
- CORBETT, S. A., LEE, L., WILSON, C. L. & SCHWARZBAUER, J. E. (1997). Covalent cross-linking of fibronectin to fibrin is required for maximal cell adhesion to fibronectin–fibrin matrix. *J. Biol. Chem.* **272**, 24 999–25 005.
- CROWE, D. L. & SHULER, C. F. (1999). Regulation of tumor cell invasion by extracellular matrix. *Histol. Histopathol.* **14**, 665–671.
- DALLON, J. C., SHERRATT, J. A. & MAINI, P. K. (1999). Mathematical modelling of extracellular matrix dynamics using discrete cells: fiber orientation and tissue regeneration. *J. theor. Biol.* **199**, 449–471.
- DAVIS, G. E., BAYLESS, K. J., DAVIS, M. J. & MEININGER, G. A. (2000). Regulation of tissue injury responses by the exposure of matricryptic sites within extracellular matrix molecules. *Am. J. Pathol.* **156**, 1489–1498.
- DECLERCK, Y. A. (2000). Interactions between tumor cells and stromal cells and proteolytic modification of the extracellular matrix by metalloproteinases in cancer. *Eur. J. Cancer* **36**, 1258–1268.
- DENIS, L. J. & VERWEIJ, J. (1997). Matrix metalloproteinase inhibitors: present achievements and future prospects. *Invest. New Drugs* **15**, 175–185.
- DI-MILLA, P. A., BARBEE, K. & LAUFFENBURGER, D. A. (1991). Mathematical model for the effects of adhesion and mechanics on cell migration speed. *Biophys. J.* **60**, 15–37.
- DOEDEL, E. J. (1981). AUTO: a program for the automatic bifurcation analysis of autonomous systems. In: *Proceedings of the 10th Manitoba Conference on Numerical Mathematics and Computation*, University of Manitoba, Winnipeg, Canada, pp. 265–284.
- DUFFY, M. J. & MCCARTHY, K. (1998). Matrix metalloproteinases in cancer: prognostic markers and targets for therapy. *Int. J. Oncol.* **12**, 1343–1348.
- DUSTIN, M. L. & de FOUGEROLLES, A. R. (2001). Reprogramming T cells: the role of extracellular matrix in coordination of T cell activation and migration. *Curr. Opin. Immunol.* **13**, 286–290.
- FERRELL, J. E. (1996). Tripping the switch fantastic: hox a protein kinase cascade can convert graded inputs into switch-like outputs. *Trends Biochem. Sci.* **21**, 460–466.
- FERREL, J. E. & MACHLEDER, E. M. (1998). The biochemical basis of an All-or-None cell fate switch in *Xenopus* Oocytes. *Science* **280**, 895–898.
- FERREL, J. E. & XIONG, W. (2001). Bistability in cell signaling: how to make continuous processes discontinuous and reversible processes irreversible. *Chaos* **11**, 227–236.
- FOLK, J. E. (1967). Mechanism of action of guinea pig liver transglutaminase VI—order of substrate addition. *J. Biol. Chem.* **244**, 3707–3713.
- FOLK, J. E., COLE, P. W. & MULLOOLY, J. P. (1969). Mechanism of action of guinea pig liver transglutaminase IV—The trimethylacyl enzyme. *J. Biol. Chem.* **242**, 4329–4333.
- GIANELLI, G., FALK-MARZILLIER, J., SCHIRALDI, O., STETLER-STEVENSON, W. G. & QUARANTA, V. (1997). Induction of cell migration by matrix metalloproteinase-2 cleavage of laminin-5. *Science* **277**, 225–228.

- GOLDBETER, A. & KOSHLAND JR, D. E. (1982). Sensitivity amplification in biochemical systems. *Q. Rev. Biophys.* **15**, 555–591.
- GONZE, D. & GOLDBETER, A. (2000). A model for a network of phosphorylation-dephosphorylation cycles displaying the dynamics of dominoes and clocks. *J. theor. Biol.* **210**, 167–186.
- GRIGORIEV, M. Y., SUSPITSIN, E. N., TOGO, A. V., POZHARISSKI, K. M., IVANOVA, O. A., NARDACCI, R., FALASCA, L., PIACENTINI, M., IMYANITOV, E. N. & HANSON, K. P. (2001). Tissue transglutaminase expression in breast carcinomas. *J. Exp. Clin. Cancer Res.* **20**, 265–268.
- GUIDI, G. M. & GOLDBETER, A. (1998). From bistability to oscillations in a model for the isocitrate dehydrogenase reaction. *Biophys. Chem.* **71**, 201–210.
- GUIDI, G. & GOLDBETER, A. (2000). Oscillations and bistability predicted by a model for a cyclical bienzymatic system involving the regulated isocitrate dehydrogenase reaction. *Biophys. Chem.* **83**, 153–170.
- HAROON, Z. A., LAI, T. S., HETTASCH, J. M., LINDBERG, R. A., DEWHIRST, M. W. & GREENBERG, C. S. (1999). Tissue transglutaminase is expressed as a host response to tumor invasion and inhibits tumor growth. *Lab. Invest.* **79**, 1679–1686.
- HAROON, Z. A., HETTASCH, J. M., LAI, T. S., DEWHIRST, M. W. & GREENBERG, C. S. (2000). Tissue transglutaminase is expressed, active and directly involved in rat dermal wound healing and angiogenesis. *FASEB J.* **13**, 1787–1794.
- HAY, E. D. (1981). Collagen and embryonic development. In: *Cell Biology of Extracellular Matrix* (Hay, E. D., ed.), pp. 379–409. New York: Plenum Press.
- HEINO, J. (1996). Biology of tumor cell invasion: interplay of cell adhesion and matrix degradation. *Int. J. Cancer* **65**, 717–722.
- HERVAGUALT, J. F. & CANU, S. (1987). Bistability and irreversible transitions in a simple substrate cycle. *J. theor. Biol.* **127**, 439–449.
- HUANG, C.-Y. & FERREL, J. E. (1996). Ultrasensitivity in the mitogen-activated protein kinase cascade. *Proc. Natl Acad. Sci. U.S.A.* **93**, 10 078–10 083.
- HULBOY, D. L., RUDOLPH, L. A. & MATRISIAN, L. M. (1997). Matrix metalloproteinases as mediators of reproductive function. *Mol. Hum. Reprod.* **3**, 27–45.
- HYNES, R. O. (1999). The dynamic dialogue between cells and matrices: implications of fibronectin's elasticity. *Proc. Natl Acad. Sci. U.S.A.* **96**, 2588–2590.
- KASAHARA, Y., ODAI, H., TAKAHASHI, K., NAGASAWA, S. & KOYAMA, J. (1985). Autocatalytic activation of C1r subcomponent of the first component of human complement. *J. Biochem.* **97**, 365–372.
- KATZ, B.-Z., ZAMIR, E., BERSHADSKY, A., KAM, Z., YAMADA, K. M. & GEIGER, B. (2000). Physical state of the extracellular matrix regulates the structure and molecular composition of cell-matrix adhesions. *Mol. Biol. Cell* **11**, 1047–1060.
- KINDZELSKII, A. L., ZHOU, M.-J., HAUGLAND, R. P., BOXER, L. A. & PETTY, H. R. (1998). Oscillatory pericellular proteolysis and oxidant deposition during neutrophil locomotion. *Biophys. J.* **74**, 90–97.
- LAFLAMME, S. E. & AUER, K. L. (1996). Integrin signaling. *Seminars Cancer Biol.* **7**, 111–118.
- LANDMAN, K. A. & PETTET, G. J. (1998). Modelling the action of proteinase and inhibitor in tissue invasion. *Math. Biosci.* **154**, 23–37.
- LAURENT, M. & KELLERSHOHN, N. (1999). Multistability: a major means of differentiation and evolution in biological systems. *Trends Biochem. Sci.* **24**, 418–422.
- LEBLANC, A., GRAVEL, C., LABELLE, J. & KEILLOR, J. W. (2001). Kinetic studies of guinea pig transglutaminase reveal a general base-catalyzed deacylation mechanism. *Biochemistry* **40**, 8335–8342.
- LIOTTA, L. A., STEEG, P. S. & STETLER-STEVENSON, W. G. (1991). Cancer metastasis and angiogenesis: an imbalance of positive and negative regulation. *Cell* **64**, 327–336.
- LISMAN, J. E. (1985). A mechanism for memory storage insensitive to molecular turnover: a bistable autophosphorylating kinase. *Proc. Natl Acad. Sci. U.S.A.* **82**, 3055–3057.
- MARIQUE, T. & WÉRENNE, J. (2001). Control of 92 kDa collagenase secretion in mammalian cells by modulation of AP-1 activity: an experimentally based theoretical study. *J. theor. Biol.* **209**, 003–008.
- MCCAWLEY, L. J. & MATRISIAN, L. M. (2000). Matrix metalloproteinases: multifunctional contributors to tumor progression. *Mol. Med. Today* **6**, 149–156.
- MCCAWLEY, L. J. & MATRISIAN, L. M. (2001). Matrix metalloproteinases: they're not just for matrix anymore! *Curr. Opin. Cell Biol.* **13**, 534–540.
- MORUGOVNA, E., TUUTILA, A., BERGMANN, U., ISUPOV, M., LINDQVIST, Y., SCHNEIDER, G. & TRYGGVASON, K. (1999). Structure of human pro-matrix metalloproteinase-2: activation mechanism revealed. *Science* **284**, 1667–1670.
- MOTOKI, M. & SEGURO, K. (1998). Transglutaminase and its use in food processing. *Trends Food Sci. Technol.* **9**, 204–210.
- MURPHY, G. & GAVRILOVIC, J. (1999). Proteolysis and cell migration: creating a path? *Curr. Opin. Cell Biol.* **11**, 614–621.
- NAKAHARA, H., HOWARD, L., THOMPSON, E. W., SATO, H., SEIKI, M., YEH, Y. & CHEN, W.-T. (1997). Transmembrane/cytoplasmic domain-mediated membrane type 1-matrix metalloprotease docking to invadopodia is required for cell invasion. *Proc. Natl Acad. Sci. U.S.A.* **94**, 7959–7964.
- NIO, N., MOTOKI, M. & TAKINAMI, K. (1986). Gelation mechanism of protein solution by transglutaminase. *Agric. Biol. Chem.* **50**, 851–855.
- OHASHI, Y., KIEHART, D. P. & ERICKSON, H. P. (1999). Dynamics and elasticity of the fibronectin matrix in living cell culture visualized by fibronectin-green fluorescent protein. *Proc. Natl Acad. Sci. U.S.A.* **96**, 2153–2158.
- PALECEK, S. P., LOFTUS, J. C., GINSBERG, M. H., LAUFENBURGE, D. A. & HORWITZ, A. F. (1997). Integrin-ligand binding properties govern cell migration speed through cell-substratum adhesiveness. *Nature* **385**, 537–540.
- PERRIS, R. & PERISSINOTTO, D. (2000). Role of the extracellular matrix during crest cell migration. *Mech. Dev.* **95**, 3–21.
- PERUMPANANI, A. J. & BYRNE, H. M. (1999). Extracellular matrix concentration exerts selection pressure on invasive cells. *Eur. J. Cancer* **35**, 1274–1280.
- PERUMPANANI, A. J., SHERRATT, J. A., NORBURY, J. & BYRNE, H. M. (1996). Biological inferences from a

- mathematical model for malignant invasion. *Invasion Metastasis* **16**, 209–221.
- PERUMPANANI, A. J., SIMMONS, D. L., GEARING, A. J. H., MILLER, K. M., WARD, G., NORBURY, J. & SHERRATT, J. A. (1998). Extracellular matrix-mediated chemotaxis can impede cell migration. *Proc. R. Soc. London B Ser.* **265**, 2347–2352.
- PERUMPANANI, A. J., SHERRATT, J. A., NORBURY, J. & BYRNE, H. M. (1999). A two parameter family of travelling waves with a singular barrier arising from the modelling of extracellular matrix mediated cellular invasion. *Physica D* **126**, 145–159.
- PRICE, J. T., BONOVIK, M. T. & KOHN, E. C. (1997). The biochemistry of cancer dissemination. *Crit. Rev. Biochem. Mol.* **32**, 175–253.
- SCHELLENBERGER, W. & HERVAGULT, J. F. (1991). Irreversible transitions in the 6-phosphofructokinase/fructose 1,6-bisphosphatase cycle. *Eur. J. Biochem.* **195**, 109–113.
- THOMAS, R. (1998). Laws for the dynamics of regulatory networks. *Int. J. Dev. Biol.* **42**, 479–485.
- THRON, C. D. (1999). Mathematical analysis of binary activation of a cell cycle kinase which down regulates its own inhibitor. *Biophys. Chem.* **79**, 95–106.
- VILLIERS, C. L., ARLAUD, G. J. & COLOMB, M. G. (1983). Autoactivation of human complement subcomponent C1r involves structural changes reflected in modifications of intrinsic fluorescence, circular dichroism and reactivity with monoclonal antibody. *Biochem. J.* **215**, 369–375.
- WEBB, S. D., SHERRATT, J. A. & FISH, R. G. (1999). Alterations in proteolytic activity at low pH and its association with invasion: a theoretical model. *Clin. Exp. Metastasis* **17**, 397–407.
- WERB, Z. (1997). ECM and cell surface proteolysis: regulating cellular ecology. *Cell* **91**, 439–442.
- WERB, Z., TREMBLE, P. M., BEHRENDTSEN, O., CROWLEY, E. & DAMSKY, C. (1989). Signal transduction through the fibronectin receptor induces collagenase and stromelysin gene expression. *J. Cell Biol.* **109**, 877–889.
- WILL, H., ATKINSON, S. J., BUTLER, G. S., SMITH, B. & MURPHY, G. (1996). The soluble catalytic domain of membrane type 1 matrix metalloproteinase cleaves the propeptide of progelatinase A and initiates autoproteolytic activation. *J. Biol. Chem.* **271**, 17 119–17 123.
- WILSON, C. L., HEPPNER, K. J., LABOSKY, P. A., HOGAN, B. L. M. & MATRISIAN, L. M. (1997). Intestinal tumorigenesis is suppressed in mice lacking the metalloproteinase matrilysin. *Proc. Natl Acad. Sci. U.S.A.* **94**, 1402–1407.
- WITTE, M. B. & BARBUL, A. (1997). General principles of wound healing. *Surg Clin. North Am.* **77**, 509–528.
- YAMADA, K. M. (1997). Integrin signaling. *Matrix Biol.* **16**, 137–141.
- ZHABOTINSKY, A. M. (2000). Bistability in the  $\text{Ca}^{2+}$ /Calmodulin-dependent protein kinase-phosphatase system. *Biophys. J.* **79**, 2211–2221.